Aromatization of propane: Techno-economic analysis by multiscale "kinetics-to-process" simulation

Michele Corbetta [a], Flavio Manenti [a,*], Carlo Pirola [b],
Mark V. Tsodikov [c], Andrey V. Chistyakov [c]

[a] Politecnico di Milano, Dipartimento di Chimica, Materiali e Ingegneria Chimica "Giulio Natta", Piazza Leonardo da Vinci, 32, 20133 Milano, Italy
[b] Università degli Studi di Milano, Dipartimento di Chimica, Via Golgi, 19, 20133 Milano, Italy
[c] A.V.Topchiev Institute of Petrochemical Synthesis, Leninskiy prospect, 29, Moscow 119991, Russian Federation

1. Introduction

The recent interest in third generation biorefineries results in an increased attention on correlated processes for the valorization of by-/co-products, which are the perquisite for a zero-waste and economic sustainable plant.

Focusing the attention on oleaginous biomass sources (e.g., microalgae), two main technological routes are adopted for the conversion of raw bio-oil to biofuels. The first one that had been developed is the transesterification to biodiesel, which is defined as the mono-alkyl esters of fatty acids (FAME) derived from triglycerides. Transesterification with an alcohol, such as methanol, occurs under mild conditions in the presence of a base catalyst and co-produces low-value glycerol, which can be subjected to aqueous-phase-reforming to produce hydrogen. Recent works show the possibility to pre-treat raw oil (broadly composed by a triglyceride mixture) with a catalytic deacidification step in order to lower the free-fatty-acids (FFA) content and to avoid soap formation in the subsequent transesterification process, starting either from waste animal fat (Bianchi et al., 2009) or raw sunflower oil (Pirola et al., 2014). The second technological route consists in a hydrodeoxygenation at high temperature and pressure in the presence of a catalyst, with the production of drop-in renewable (green) diesel and hydrotreated renewable jet (HRJ) fuels. Hydroprocessing is employed in conventional refinery processes to firstly deoxygenate and remove undesirable materials including nitrogen, sulphur and residual metals and break down carbon chain lengths. Similarly, the biomass synthetic jet fuel production process involves removing oxygen molecules and other undesirable materials from triglycerides through hydrotreatment, and a subsequent selective hydrocracking/rearrangement of the atomic structure to yield lighter hydrocarbons suitable for aviation (Jet A-1: C8–C16) (Blakey et al., 2011). These catalytic processes determine the cracking of triglycerides, saturation of double bonds, heteroatoms rejection and isomerization. The main difference between biodiesel and green diesel consists in their chemical characterization. Green diesel is a drop-in fuel with a chemical structure similar to the petro-derived diesel irrespective of the feedstock and without oxygen content, which is not true for biodiesel (Knothe, 2010). HRJ fuel is substantially composed by a pool of long chain paraffins free from aromatics compounds. As a consequence, HRJ fuel meets the world jet fuel specifications (ExxonMobil Aviation, 2005) for the threshold value of 25 vol% of aromatics in the Jet A-1 category.

---

* Corresponding author. Tel.: +39 0 2 2399 3273; fax: +39 0 2 2399 3280.
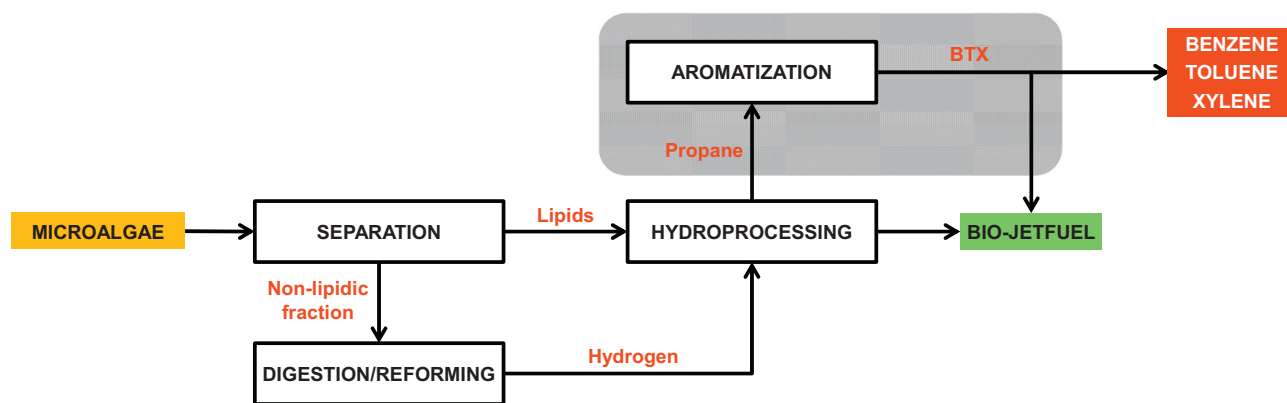 E-mail address: flavio.manenti@polimi.it (F. Manenti).

Fig. 1. Blocks diagram of a possible third generation zero-waste biorefinery.

According to Blakey and co-workers, one of the biggest concerns of alternative fuels has come from their low aromatic content. Concern has been raised that the ageing seals in the aircraft and engine would leak if the aromatic content is too low, as the seals would shrink. For this reason the aromatic content of synthetic fuel blends is currently fixed at a minimum of 8% (Blakey et al., 2011). On the other hand, Hui and co-workers studied the ignition and combustion of alternative jet fuels and they found that cetane numbers (CN) are higher than that of Jet-A. This is because Jet-A contains about 20% aromatics while HRJ consists mostly of iso-paraffin and cyclo-paraffin, which are less reactive compared to n-paraffins (Hui et al., 2012).

A strategy to produce HRJ fuel that satisfies this requirement is to blend it with aromatics produced from bio-based propane aromatization. The resulting integrated third generation biorefinery is illustrated in Fig. 1. This concept consists in a main hydroprocessing step of the algal oil, derived from the separation between the lipid and non-lipid fractions of the harvested microalgae. During this catalytic conversion, HRJ fuels are produced along with propane. This co-product is then aromatized over H-ZSM-5 catalyst to produce aromatics for blending and for sale on the petrochemical market. Unfortunately the selectivity towards high-value aromatics is reduced by the significant co-production of fuel gas (methane and ethane), which has a lower economic value. In general, zeolites with MFI pore structure are used, due to their high resistance to deactivation. Additionally, metal components, such as gallium, could be added to enhance the dehydrogenation function.

Nguyen and co-workers performed experimental and modelling studies of propane and n-butane aromatization over H-ZSM-5 zeolite at 500 °C in a wide range of conversions (Nguyen et al., 2006). Analysis of the experimental and kinetic modelling data has confirmed that propane and n-butane transformation over H-ZSM-5 occurs via both protolytic cracking of C—C and C—H bonds in paraffin molecules and hydrogen transfer between the propane and product olefins adsorbed on acid sites. Light olefins formed in the initial reaction steps give rise to fast oligomerization/cracking steps that control olefin distribution, as demonstrated in both the mechanistic studies of ethene and propene aromatization (Lukyanov et al., 1994) and propane aromatization (Lukyanov et al., 1994). Reaction kinetic studies of propane catalytic conversion to aromatics were also conducted by Bhan and co-workers on the same catalyst at atmospheric pressure and temperatures in the range of 520–550 °C, and different space times (Bhan et al., 2005). The same authors proposed additional investigations on the role of gallium modified zeolites (Bhan and Nicholas Delgass, 2008). The rates of production of several species are reported in both papers. They developed a kinetic model considering surface species as neutral alkoxides, reactions of these alkoxide species

by carbenium ion-like transition states, and alkane activation by carbonium ion-like transition states.

Going further on, beyond the kinetic modelling and towards the plant scale, it should be noted that a global chemical process (e.g., propane aromatization process) consists of complex systems occurring at different levels, each with its own unique multi-scale structure (Li et al., 2005). The lack of commercial software able to integrate all these multidisciplinary features (Charpentier, 2009) drives the research towards the integration of different tools targeting different scales. Process System Engineering (PSE) provides numerical tools and platforms devoted to the investigation of the so-called Chemical Supply-Chain (Grossmann and Westerberg, 2000), which spans from the science-oriented study at the molecular level up to the system-oriented study of process networks and beyond.

This work proposes a new kinetic mechanism (micro and reactor scales) of propane aromatization, which is embedded in a multi-scale process simulation (process scale). The process simulation is performed with the PRO/II process modelling environment (PME), which has been extensively adopted both in the industrial and in the academic practice to model process plants that do not yet exist and to evaluate their economic viability (Lam et al., 2011). The necessity to include a custom process modelling component (PMC) derives from the choice of describing the catalytic reactor with a detailed surface kinetic mechanism. In the literature (Morales-Rodríguez and Gani, 2007) many efforts have been devoted to the definition of an efficient computer-aided framework to integrate PMCs in PMEs. For instance, the CAPE-OPEN standard has been widely adopted and integrated within PMEs. Applications of CAPE-OPEN standard in the field of PSE include, for instance, the modelling of thermodynamic properties and the modelling of new unit operations (Morales-Rodríguez et al., 2008). In both cases, the bridging between PMC and PME is obtained by a proper Middleware (e.g., CORBA, COM, .NET Framework).

The novelty of this work relies on the use of a different standard and Middleware. Particularly, Microsoft Excel is adopted to manage all communications between the PRO/II PME and the PMC (catalytic reactor unit), as outlined in Fig. 2. The advantage of this approach derives from its easiness and usability. In fact, home-made codes developed by engineers during R&D activities (e.g., regression of kinetic and thermodynamic models) could by directly embed within process simulators without the need for further modifications. Moreover, the use of the excel unit operation module allows directly post-processing and reporting simulation results in tables and graphs.

Section 2 addresses the reactor and kinetic modelling of propane aromatization on H-ZSM-5 catalysts; Section 3 shows results of the process simulation of the Cyclar process, performed
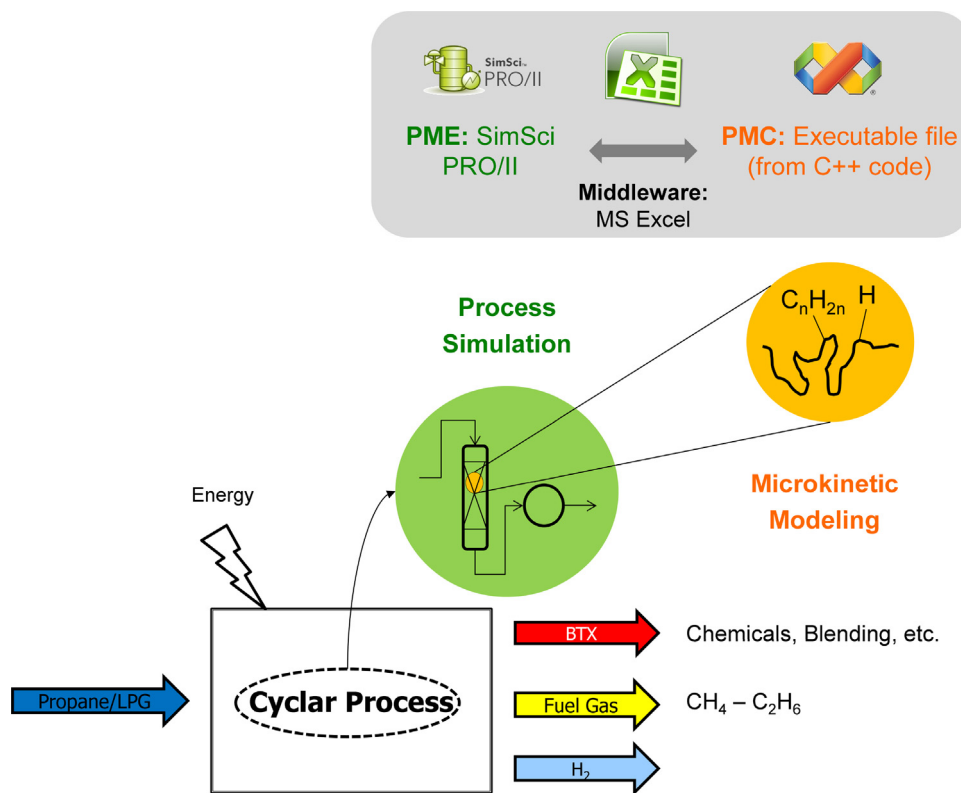
Fig. 2. Logical blocks of the multiscale approach applied to the aromatization process.

with the commercial code SimSci PRO/II by Schneider Electric; Section 4 reports some economic considerations; and finally Section 5 includes results and general comments.

2. Kinetic modelling

The reactive system has been modelled considering the following 19 chemical species and lumps. For instance, paraffin C6 includes all the saturated chain isomers with six carbon atoms.

It is worth mentioning that other chemical species (i.e., alkyl-cyclohexanes, alkyl-cyclohexadienes, etc.) are observed just in traces and for this reason they are not taken into account in the model. These intermediates species participate in the fast sub-steps of the aromatization of large olefins.

The chemical species listed in Table 1 are involved in several reactive steps, which could be categorized in 5 reactions classes, plus adsorption and desorption steps. The reaction pathway is illustrated in Fig. 3. Accordingly, paraffins are activated on acid sites by protolytic cracking or dehydrogenation, being the first route roughly 2.5 times faster. Once olefins are produced, they can rapidly oligomerize yielding heavier olefins (Buchanan et al., 1996), which, in turn, can activate paraffins with H-transfer reactions (Kazansky et al., 1997), or aromatize with other olefins, evolving the corresponding paraffins.

Stoichiometries are generated according with the following rules, while the full set of reactions (79 reactions), along with kinetic parameters, is reported in Appendix 1.

Table 1
Chemical species and lumps.

Hydrogen	H_2	1
Paraffins	$CH_4-C_8H_{18}$	8
Olefins	$C_2H_4-C_8H_{16}$	7
Aromatics	B/T/X	3
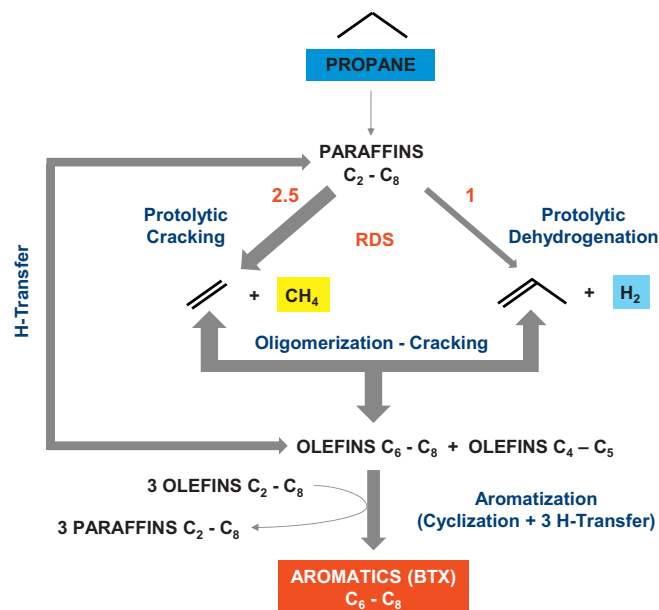
Fig. 3. Reaction pathways.

2.1. Adsorption/desorption on acid sites (Zeolite HZSM-5)

Olefins	$C_n^=$	$C_n^= \leftrightarrow (C_n^=)^*$
Aromatics	A_n	$A_n \leftrightarrow (A_n)^*$

Adsorption and desorption steps are considered at equilibrium because they are faster than the other reactive steps (Lukyanov et al., 1995). As a consequence, each reaction is characterized by only one parameter (adsorption constant, K_{ads}).

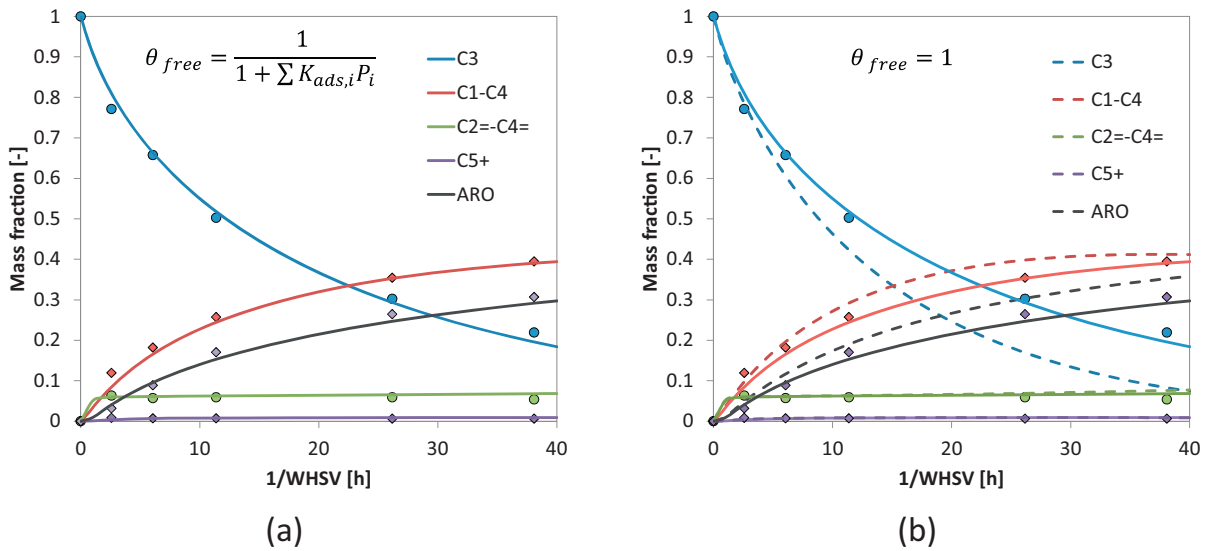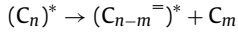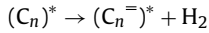$$\theta_i^* = K_{ads,i} P_i \theta_{lib} \quad [-]$$

Fig. 4. Comparisons of model simulations and experimental data (Nguyen et al., 2006). Panel (a): full model. Panel (b): comparison between the full model (solid line) and the power law model without adsorption.

2.2. Activation of paraffins on acid sites (Zeolite HZSM-5)
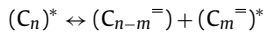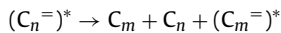
(a) Protolytic cracking

$$(C_n)^* \rightarrow (C_{n-m}^=)^* + C_m$$

(b) Protolytic dehydrogenation

$$(C_n)^* \rightarrow (C_n^=)^* + H_2$$

2.3. Reactivity of insaturated on acid sites (Zeolite HZSM-5)

a. B-Scission/oligomerization

$$(C_n)^* \leftrightarrow (C_{n-m}^=) + (C_m^=)^*$$

b. H-Transfer

$$(C_n^=)^* \rightarrow C_m + C_n + (C_m^=)^*$$

c. Aromatization

$$(C_m^=)^* + 3\,C_n^= \rightarrow 3\,C_n + (A_m)^*$$
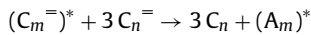
The mathematical model of the catalytic system consists in a PFR isothermal pseudo-homogeneous reactor model with reaction rates evaluated according with the Eley–Rideal (E–R) surface kinetic mechanism. Eq. (1) reports the material balance for the i-th species, in which ω represents its mass fraction and τ is the reciprocal of the weight hourly space velocity (WHSV = total mass flow/catalyst mass load). E–R reaction rates of Eq. (2) reflect the saturation effect of olefins and aromatics adsorbed on surface active sites. Finally, kinetic constants ($k_{KIN,j}$) are considered with an Arrhenius expression.

$$\frac{d\omega_i}{d\tau} = r_i MW_i = \sum_{j=1}^{Nreact} \nu_{i,j} r_j MW_i \tag{1}$$

$$r_j = k_{KIN,j} \frac{\displaystyle\prod_{m=1}^{Nreact} P_m}{1 + \displaystyle\prod_{n=1}^{Nads} K_{ADS,n} P_n} \tag{2}$$

$$k_{KIN,j} = A_j \cdot \exp\left(-\frac{E_{act,j}}{RT}\right) \tag{3}$$

Regression of kinetic parameters (Buzzi-Ferraris and Manenti, 2009) has been performed by means of the set of very robust optimizers belonging to the BzzMath library (Buzzi-Ferraris and Manenti, 2012). The library is available at http://super.chem.polimi.it/. Such optimizers are based on the object-oriented programming and parallel computing, leading to a reduction of the computational time. BzzMath library includes special numerical methods able to simultaneously handle the so-called narrow-valley problem, which typically arise from the estimation of kinetic and thermodynamic parameters, the possible multicollinearities, which could be due to coupled chemical-physical phenomena, and the possible presence of bad-quality measures with the identification of outliers.

The nonlinear regression has been accomplished minimizing the objective function of Eq. (4), using experimental data from the available literature (Nguyen et al., 1995). The objective function is a weighed ($\omega_{i,k}$) least sum of square errors, in which $g_k(\boldsymbol{x}_i, \boldsymbol{b})$ is the model prediction of the k-th dependent variable, as a function of independent variables ($\boldsymbol{x}_i$) and model parameters ($\boldsymbol{b}$).

$$S(\boldsymbol{b}) = \sum_{i=1}^{N\exp} \sum_{k=1}^{Ny} \left[\omega_{i,k}(y_{i,k} - g_k(\boldsymbol{x}_i, \boldsymbol{b}))\right]^2 \tag{4}$$

Model predictions are compared with experimental data in Fig. 4. Note that the model nicely fits experimental data of species mass fractions as a function of WHSV. Propane is progressively converted to two main products, which are aromatics and fuel gas (essentially methane and ethane). Experimental aromatics distribution has an average trend of 26/51/23 wt.% in B/T/X (Giannetto et al., 1994), which is well reproduced by the kinetic model. C5+ products, comprising all species with at least 5 carbon atoms, are found in small amounts, while $C_2^=$–$C_4^=$ product composition is almost constant in the range of 7 wt.%. Panel (b) shows the model

Table 2
Global material balances.

Stream	Mass flowrate [t/h]	Molar flowrate [kmol/h]	Mass fraction of the key component [−]
Propane (feed)	4.410	100	1.00
Fuel gas C_2H_6 – CH_4 (70–30% mol)	0.790	29.7	0.78
CH_4 – H_2 – C_2H_6 (60–30–10% mol)	1.820	134	0.69
Benzene	0.484	6.20	0.97
Toluene	0.910	9.91	0.96
Xylene	0.396	3.74	0.99
Purge (propane – benzene)	0.010	0.21	0.40

$$\theta_{A*} = \frac{K_{ads,A}P_A}{1 + \sum_i K_{ads,i}P_i}$$

Fig. 5. Model prediction of surface coverage by olefins and aromatics.

Table 3
Reactor specifications.

		Specification
Reactor temperature	[°C]	500
Reactor pressure	[bar]	1.2
Catalyst load	[t]	325
Propane conversion (mass)	[−]	0.900
BTX yield (mass)	[−]	0.373

amount of light olefins (C2=–C4=). Finally, the sensitivity of product distribution on aromatization rates appears to be negligible.

3. Multiscale process simulation

Once the kinetic scheme has been validated against experimental data, it has been corroborated with a process simulation. The BP/UOP Cyclar aromatization process has been selected and simulated by means of the commercial code PRO/II (Fig. 7).

The Cyclar process is composed by a catalytic section and a downstream section. The propane feed enters the catalytic reactor after a mixing step with the unconverted and recycled propane. Industrially, the reactor is a multiple inter-heated adiabatic annular moving-bed catalytic reactor. This unit has been simulated with a custom model, exploiting the excel unit operation module. In this way, the process simulator (PME) calls a Microsoft Excel file (Middleware) with a Visual Basic macro that executes a reactor model routine (PMC) with the detailed kinetic model previously reported. The reactor effluent enters a feed-effluent-heat-exchanger (FEHE) and it is compressed and sent to a separator.

In the downstream section, the gas phase is further compressed and fed to a de-ethanizer, where the cut between ethane and propane is realized. Propane and heavies are recycled, while in the partial condenser a liquid stream rich in ethane (with methane) and a gas stream rich in methane (with hydrogen) are withdrawn. The liquid stream effluent from the flash is pumped to a stabilizer, where light hydrocarbons are stripped from the top and recycled to the catalytic section. From the bottom of the stabilizer, a liquid stream mainly composed of aromatics is fed to the last two purification columns. The first tower separates benzene from the top, while the last one separates toluene and xylene.

The material balances and the global performances of the plant are reported in Table 2, while in Table 3 and Table 4 reactor and distillation columns specifications are summarized respectively.

results considering a power-law model (i.e., neglecting the denominator of Eq. (2), corresponding to the saturation effect), which overestimate the conversion of propane to aromatics and fuel gas. Moreover, surface coverage of active sites (Fig. 5) could be useful to understand the surface reaction mechanism, highlighting the role of the different adsorbed species on the saturation of the catalyst, as outlined in recent spectrokinetic analysis (Visconti et al., 2013) and in surface reactive CFD simulations (Corbetta et al., 2014). From Fig. 5, we can notice that aromatics are largely responsible for the coverage, with an asymptotic value of about 80%. This is due both to the fact that aromatics adsorption constant is five times greater than the olefins one, and to the low partial pressures of olefins.

Once the kinetic scheme has been validated, a sensitivity analysis on kinetic constants has been performed, in order to find out the role of the different reaction classes on the catalytic conversion process (Fig. 6). The sensitivity analysis has been carried on by multiplying by ten all the reaction rates belonging to the same class. From this parametric study emerges that protolytic cracking/dehydrogenation is the limiting step, and it determines the highest sensitivity to product distribution. Its reaction rate is the smallest one (about 1000 times smaller than other reactions). Increasing H-transfer rates results in a higher conversion of propane to light paraffins. On the other hand, oligomerization and cracking reaction classes do not affect the conversion of propane but slightly change the product distribution, mainly decreasing the

Table 4
Distillation columns specifications.

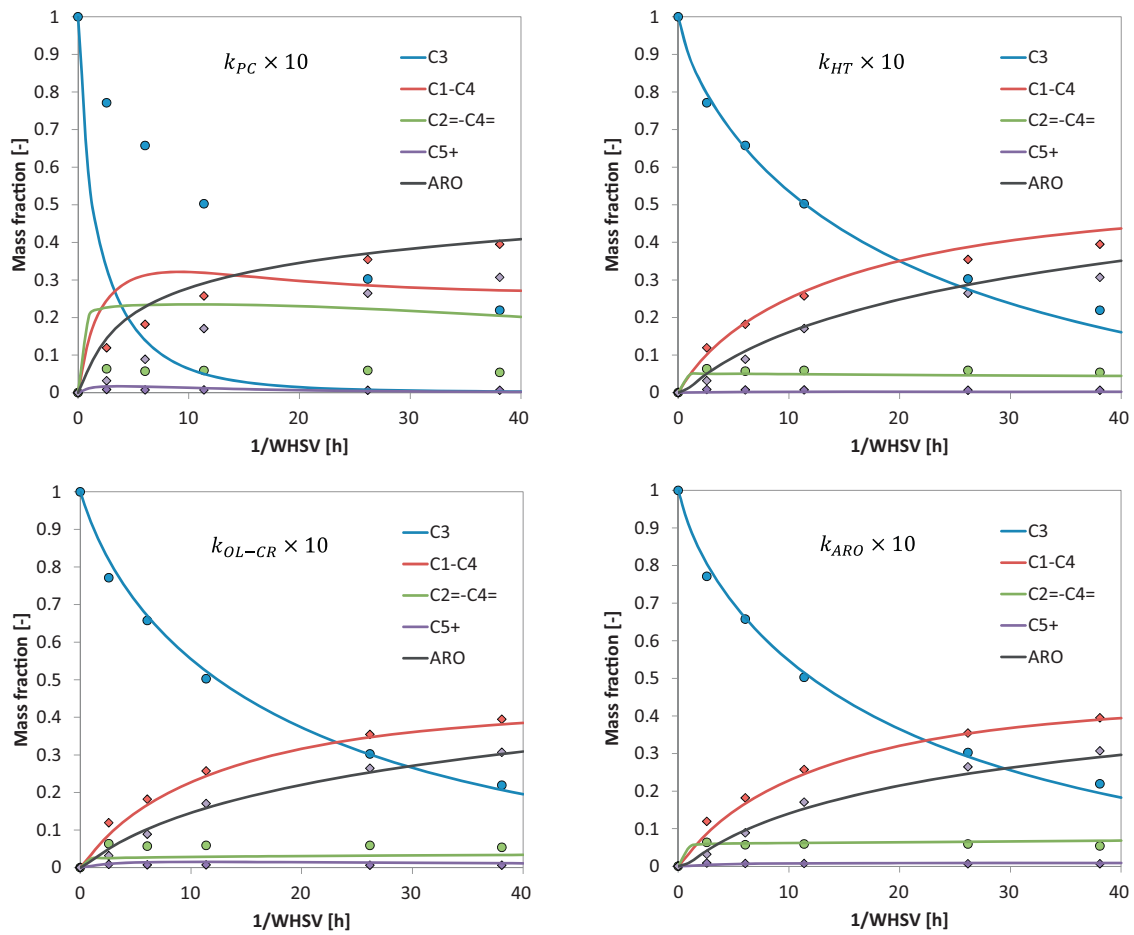|		De-ethanizer	Stabilizer	Benz-distill	TX-splitter
Number of trays	[−]	30	9	17	30
Condenser pressure	[bar]	20	10	1.2	1.2
Condenser temperature	[°C]	−74	−78	49	115
Condenser duty	[kW]	−491	−23	−555	−214
Reboiler duty	[kW]	57	134	572	215
Reflux ratio	[−]	0.6	1	Total	1.32

Fig. 6. Sensitivity analysis on reaction class kinetic constants.

The simulation has been carried on with a SRK thermodynamic package, optimizing some process parameters (feed trays, number of stages, etc.) by minimizing heat duties. The resulting liquid molar fraction profiles inside the 4 columns (de-ethanizer, stabilizer, B-distiller, and TX-splitter) are reported in Fig. 8.

4. Economic considerations

On the basis of the detailed process simulation, some economic consideration is discussed below. First of all, prices of the involved chemicals have been collected from the Platts
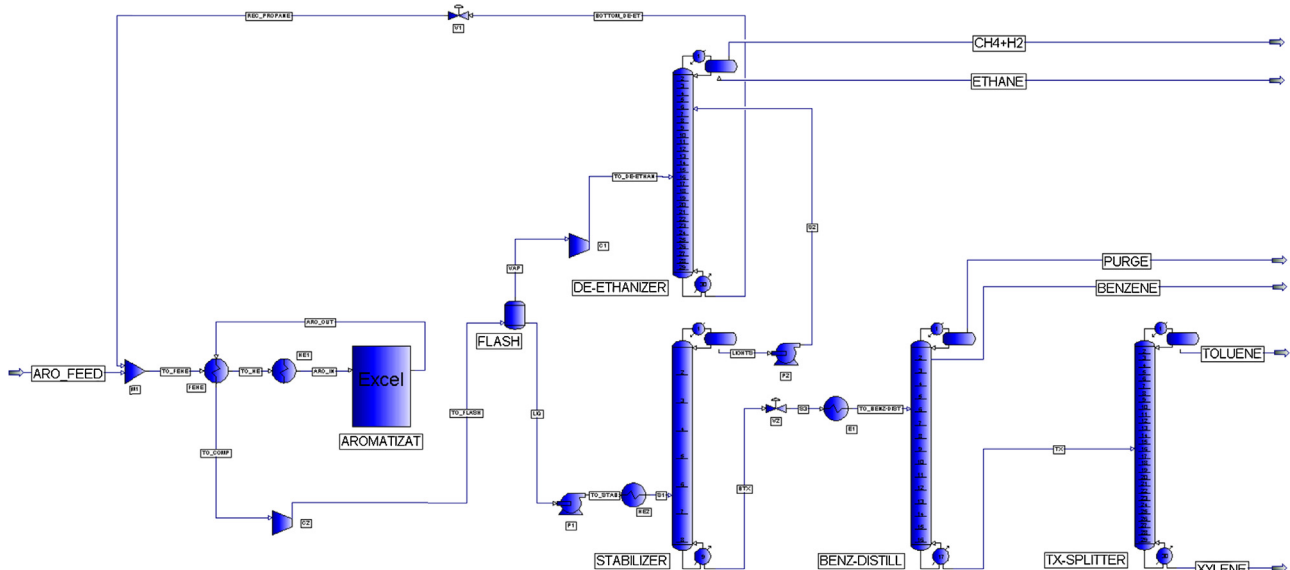

Fig. 7. Cyclar process layout adopted in the simulation.
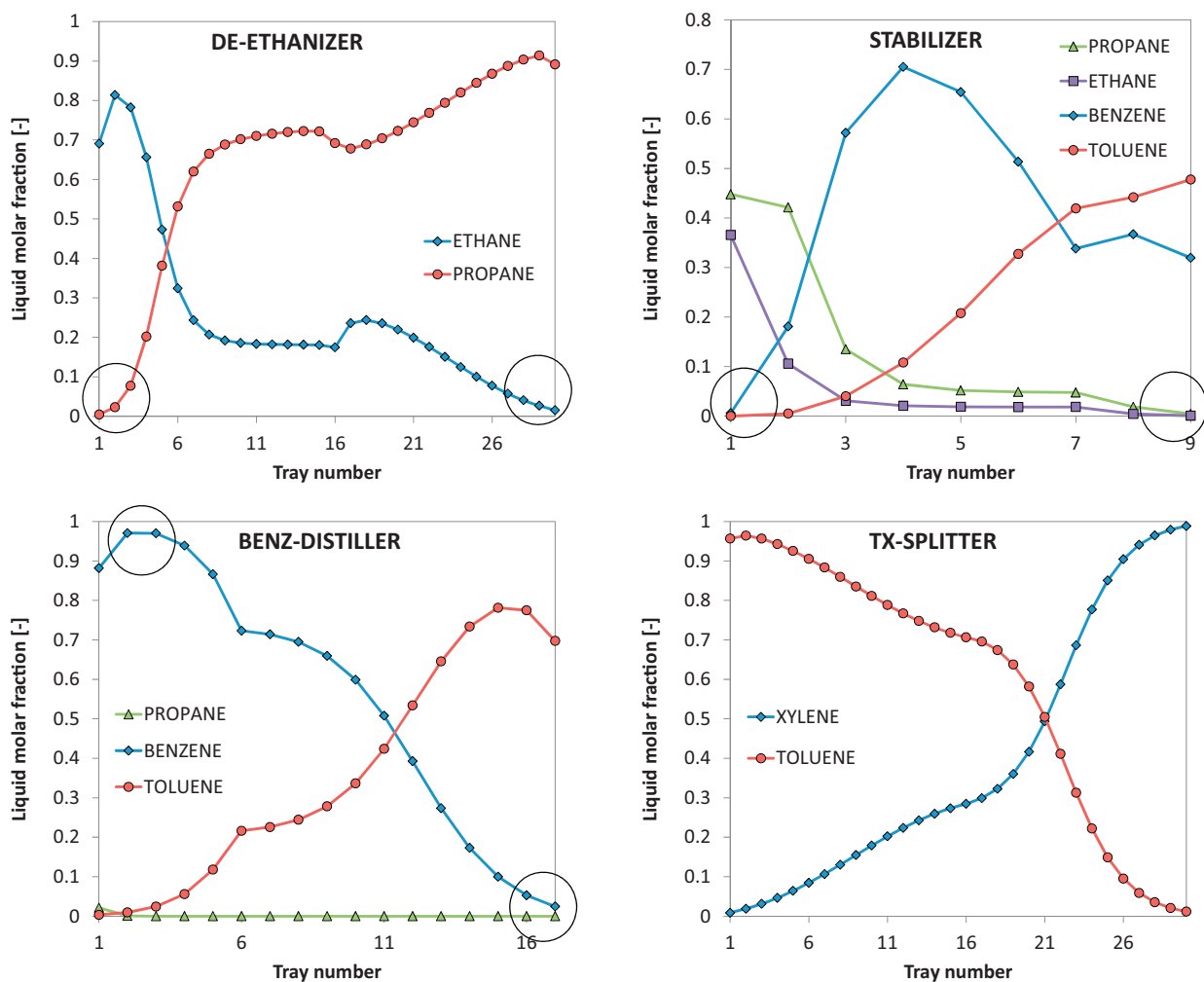
Fig. 8. Liquid composition profiles of the four distillation columns (purity specifications are highlighted with circles).

database (Table 5), a leading global provider of energy, petrochemicals, metals and agriculture information, and a premier source of benchmark price assessments for those commodity markets (Platts, 2014). In this study, annual average values of 2013 have been adopted. The typical fluctuation of petrochemical prices

is highlighted in Fig. 9, where the Platts Global Petrochemical Index (PGPI) is reported for Toluene in the period May 2013–July 2014.

Bulk chemicals prices show a significant fluctuation, and, according with the process yields, supported by experimental data,

Fig. 9. Platts global petrochemical index (PGPI) for Toluene in the period June 2013–July 2014 (Platts, 2014).

Table 5
Economic parameters.

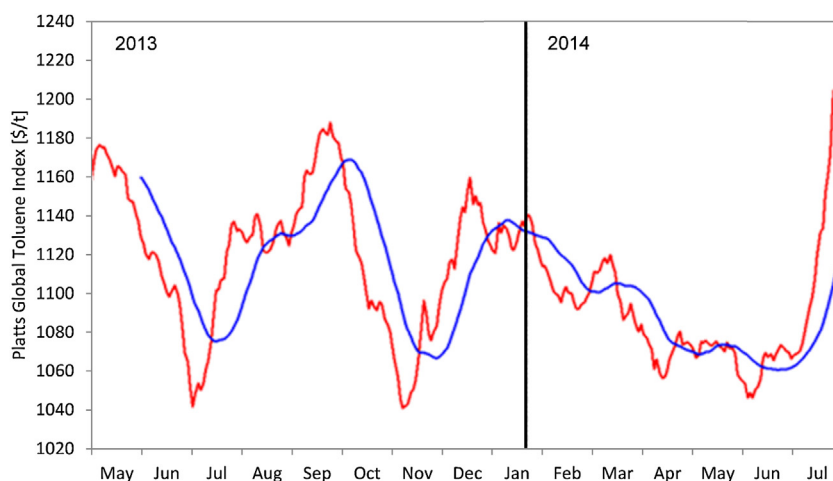| Chemical compound	Unit cost/price [€/kg]	Economic flux [€/h]	Refs.
Propane	0.599	−2641.6	Platts (2014)
Ethane	0.022	17.38	Platts (2014)
Methane	0.058	101.3	Platts (2014)
Hydrogen	1.45	105.56	Doty (2004)
Benzene	0.982	475.3	Platts (2014)
Toluene	0.941	856.3	Platts (2014)
Xylene	1.165	461.3	Platts (2014)

the global second order economic potential results in a negative value.

$$EP_2 = \sum_{j=1}^{NP} €_{P,j} n_j - \sum_{i=1}^{NR} €_{R,i} n_i < 0 \tag{5}$$

This is due to the fact that large amounts of fuel gas are co-produced along with the main BTX material stream. In fact, once methane and ethane are produced by cracking reactions, they are not anymore catalytically active on H–ZSM-5 zeolites. This evidence suggests that new catalysts should be developed in order to turn the aromatization process into economic sustainability, by increasing the selectivity towards aromatics. Catalysts with a higher selectivity towards aromatics (up to 80%) are reported in the literature (Wang et al., 2002), which are also active in methane aromatization (Shu et al., 1999), thus reducing the amount of fuel gas. By doing some rough consideration on prices, propane price is about 0.6 €/kg, BTX 1 €/kg and fuel gas 0.04 €/kg (global average prices in 2013). Consequently, to have a positive economic balance, the reactor should yield at least 60 wt.% in aromatics.

5. Conclusions

A completely new methodology to face the relevant issue of economic and industrial feasibility of process layouts in the area of biorefineries has been developed and applied to a specific case study. The methodology allowed to integrate and exploit at best all the information relating to the modelling of chemical kinetics, surface kinetics, chemical reactors, and chemical process modelling, providing an aprioristic reliable assessment of the techno-economic benefits for novel and innovative biomass conversion pathways. This approach relies on the use of Microsoft Excel as Middleware between the PRO/II PME and the PMC of custom unit operations, resulting in a flexible and easy-to-use tool.

The paper proposes a comprehensive study for the propane aromatization process specifically addressed to the integration within a third generation (microalgae) biorefinery concept. Such integration allows to overcome main concerns that have been arisen by scientists and technicians about the absence of aromatics in HRJ fuels. Moreover, the proposed solution does not imply the consumption of fossil fuels.

In order to assess this technological route, a multiscale process simulation has been proposed, relying on detailed surface kinetics. The kinetic scheme has been tuned with available experimental data by means of nonlinear regression, and the full mechanism, along with kinetic constants, is here provided. Basing on the process simulation, some economic considerations have been argued. A minimum of about 60 wt.% in aromatics' yield is necessary for economic sustainability, thus requiring further efforts on more selective catalysts development.

Appendix 1.

The kinetic scheme is reported below (Table A1) along with pre-exponential factors and activation energies. The kinetic scheme is also available at the section download of the website http://super.chem.polimi.it in CHEMKIN format.

Table A1
Kinetic scheme of propane aromatization over H–ZSM-5 catalyst. Activation energies are adapted from Bhan et al. (2005).

#	Reaction	Pre-exponential factor [mol/g/h/Pa] or [mol/g/h/Pa^2]	Activation energy [J/mol]
	Protolytic C—H Cracking		
1	$C_2H_6 > C_2H_4 + H_2$	21.302	142,000
2	$C_3H_8 > C_3H_6 + H_2$	21.302	142,000
3	$C_4H_{10} > C_4H_8 + H_2$	93.729	142,000
4	$C_5H_{12} > C_5H_{10} + H_2$	93.729	142,000
5	$C_6H_{14} > C_6H_{12} + H_2$	93.729	142,000
6	$C_7H_{16} > C_7H_{14} + H_2$	93.729	142,000
7	$C_8H_{18} > C_8H_{16} + H_2$	93.729	142,000
	Protolytic C—C Cracking		
8	$C_3H_8 > C_2H_4 + CH_4$	71.8881	142,000
9	$C_4H_{10} > C_2H_4 + C_2H_6$	186.909	142,000
10	$C_4H_{10} > C_3H_6 + CH_4$	186.909	142,000
11	$C_5H_{12} > C_2H_4 + C_3H_8$	186.909	142,000
12	$C_5H_{12} > C_3H_6 + C_2H_6$	186.909	142,000
13	$C_5H_{12} > C_4H_8 + CH_4$	186.909	142,000
14	$C_6H_{14} > C_2H_4 + C_4H_{10}$	186.909	142,000
15	$C_6H_{14} > C_3H_6 + C_3H_8$	186.909	142,000
16	$C_6H_{14} > C_4H_8 + C_2H_6$	186.909	142,000
17	$C_6H_{14} > C_5H_{10} + CH_4$	186.909	142,000
18	$C_7H_{16} > C_2H_4 + C_5H_{12}$	186.909	142,000
19	$C_7H_{16} > C_3H_6 + C_4H_{10}$	186.909	142,000
20	$C_7H_{16} > C_4H_8 + C_3H_8$	186.909	142,000
21	$C_7H_{16} > C_5H_{10} + C_2H_6$	186.909	142,000
22	$C_7H_{16} > C_6H_{12} + CH_4$	186.909	142,000

Table A1 (*Continued*)

#	Reaction	Pre-exponential factor [mol/g/h/Pa] or [mol/g/h/Pa^2]	Activation energy [J/mol]
23	$C_8H_{18} > C_2H_4 + C_6H_{14}$	186.909	142,000
24	$C_8H_{18} > C_3H_6 + C_5H_{12}$	186.909	142,000
25	$C_8H_{18} > C_4H_8 + C_4H_{10}$	186.909	142,000
26	$C_8H_{18} > C_5H_{10} + C_3H_8$	186.909	142,000
27	$C_8H_{18} > C_6H_{12} + C_2H_6$	186.909	142,000
28	$C_8H_{18} > C_7H_{14} + CH_4$	186.909	142,000
	H-Transfer		
29	$C_3H_8 + C_2H_4 > C_3H_6 + C_2H_6$	2.891e−007	86,000
30	$C_3H_8 + C_4H_8 > C_3H_6 + C_4H_{10}$	2.891e−007	86,000
31	$C_3H_8 + C_5H_{10} > C_3H_6 + C_5H_{12}$	2.891e−007	86,000
32	$C_3H_8 + C_6H_{12} > C_3H_6 + C_6H_{14}$	2.891e−007	86,000
33	$C_3H_8 + C_7H_{14} > C_3H_6 + C_7H_{16}$	2.891e−007	86,000
34	$C_3H_8 + C_8H_{16} > C_3H_6 + C_8H_{18}$	2.891e−007	86,000
35	$C_4H_{10} + C_2H_4 > C_4H_8 + C_2H_6$	2.891e−007	86,000
36	$C_4H_{10} + C_3H_6 > C_4H_8 + C_3H_8$	2.891e−007	86,000
37	$C_4H_{10} + C_5H_{10} > C_4H_8 + C_5H_{12}$	2.891e−007	86,000
38	$C_4H_{10} + C_6H_{12} > C_4H_8 + C_6H_{14}$	2.891e−007	86,000
39	$C_4H_{10} + C_7H_{14} > C_4H_8 + C_7H_{16}$	2.891e−007	86,000
40	$C_4H_{10} + C_8H_{16} > C_4H_8 + C_8H_{18}$	2.891e−007	86,000
	Oligomerization		
41	$C_2H_4 + C_2H_4 > C_4H_8$	0.001713	125,000
42	$C_2H_4 + C_3H_6 > C_5H_{10}$	0.029116	125,000
43	$C_2H_4 + C_4H_8 > C_6H_{12}$	0.056518	125,000
44	$C_2H_4 + C_5H_{10} > C_7H_{14}$	0.056518	125,000
45	$C_2H_4 + C_6H_{12} > C_8H_{16}$	0.056518	125,000
46	$C_3H_6 + C_3H_6 > C_6H_{12}$	0.061656	125,000
47	$C_3H_6 + C_4H_8 > C_7H_{14}$	0.272315	125,000
48	$C_3H_6 + C_5H_{10} > C_8H_{16}$	0.395628	125,000
49	$C_4H_8 + C_4H_8 > C_8H_{16}$	0.395628	125,000
	Cracking		
50	$C_4H_8 > C_2H_4 + C_2H_4$	1.03774	125,000
51	$C_5H_{10} > C_2H_4 + C_3H_6$	17.6416	125,000
52	$C_6H_{12} > C_2H_4 + C_4H_8$	34.2455	125,000
53	$C_7H_{14} > C_2H_4 + C_5H_{10}$	34.2455	125,000
54	$C_8H_{16} > C_2H_4 + C_6H_{12}$	34.2455	125,000
55	$C_6H_{12} > C_3H_6 + C_3H_6$	37.3587	125,000
56	$C_7H_{14} > C_3H_6 + C_4H_8$	165.001	125,000
57	$C_8H_{16} > C_3H_6 + C_5H_{10}$	239.719	125,000
58	$C_8H_{16} > C_4H_8 + C_4H_8$	239.719	125,000
	Aromatization		
59	$C_6H_{12} + 3 C_2H_4 > B + 3 C_2H_6$	8.85e−009	30,000
60	$C_7H_{14} + 3 C_2H_4 > T + 3 C_2H_6$	1.22e−005	30,000
61	$C_8H_{16} + 3 C_2H_4 > X + 3 C_2H_6$	2.21e−008	30,000
62	$C_6H_{12} + 3 C_3H_6 > B + 3 C_3H_8$	3.54e−007	30,000
63	$C_7H_{14} + 3 C_3H_6 > T + 3 C_3H_8$	0.000486	30,000
64	$C_8H_{16} + 3 C_3H_6 > X + 3 C_3H_8$	8.85e−007	30,000
65	$C_6H_{12} + 3 C_4H_8 > B + 3 C_4H_{10}$	8.85e−007	30,000
66	$C_7H_{14} + 3 C_4H_8 > T + 3 C_4H_{10}$	0.001217	30,000
67	$C_8H_{16} + 3 C_4H_8 > X + 3 C_4H_{10}$	2.21e−006	30,000
68	$C_6H_{12} + 3 C_5H_{10} > B + 3 C_5H_{12}$	8.85e−007	30,000
69	$C_7H_{14} + 3 C_5H_{10} > T + 3 C_5H_{12}$	0.001217	30,000
70	$C_8H_{16} + 3 C_5H_{10} > X + 3 C_5H_{12}$	2.21e−006	30,000
71	$C_6H_{12} + 3 C_6H_{12} > B + 3 C_6H_{14}$	8.85e−007	30,000
72	$C_7H_{14} + 3 C_6H_{12} > T + 3 C_6H_{14}$	0.001217	30,000
73	$C_8H_{16} + 3 C_6H_{12} > X + 3 C_6H_{14}$	2.21e−006	30,000
74	$C_6H_{12} + 3 C_7H_{14} > B + 3 C_7H_{16}$	8.85e−007	30,000
75	$C_7H_{14} + 3 C_7H_{14} > T + 3 C_7H_{16}$	0.001217	30,000
76	$C_8H_{16} + 3 C_7H_{14} > X + 3 C_7H_{16}$	2.21e−006	30,000
77	$C_6H_{12} + 3 C_8H_{16} > B + 3 C_8H_{18}$	8.85e−007	30,000
78	$C_7H_{14} + 3 C_8H_{16} > T + 3 C_8H_{18}$	0.001217	30,000
79	$C_8H_{16} + 3 C_8H_{16} > X + 3 C_8H_{18}$	2.21e−006	30,000

References

Bhan A, Nicholas Delgass W. Propane aromatization over HZSM-5 and Ga/HZSM-5 catalysts. Catal Rev 2008;50(1):19–51.

Bhan A, Hsu SH, Blau G, Caruthers JM, Venkatasubramanian V, Delgass WN. Microkinetic modeling of propane aromatization over HZSM-5. J Catal 2005;235(1):35–51.

Bianchi CL, Boffito DC, Pirola C, Ragaini V. Low temperature de-acidification process of animal fat as a pre-step to biodiesel production. Catal Lett 2009;134:179–85.

Blakey S, Rye L, Wilson CW. Aviation gas turbine alternative fuels: a review. Proc Combust Inst 2011;33(2):2863–85.

Buchanan JS, Santiesteban JG, Haag WO. Mechanistic considerations in acid-catalyzed cracking of olefins. J Catal 1996;158(1):279–87.

Buzzi-Ferraris G, Manenti F. BzzMath: library overview and recent advances in numerical methods. Comput Aided Chem Eng 2012;30(2):1312–6.

Buzzi-Ferraris G, Manenti F. Kinetic models analysis. Chem Eng Sci 2009;64(5):1061–74.

Charpentier JC. Perspective on multiscale methodology for product design and engineering. Comput Chem Eng 2009;33(5):936–46.

Corbetta M, Manenti F, Visconti CG. CATalytic – Post Processor (CAT – PP): a new methodology for the CFD-based simulation of highly diluted reactive heterogeneous systems. Comput Chem Eng 2014;60:76–85.

Doty FD. A realistic look at hydrogen price projections. In: Doty Scientific Inc., Technical Report; 2004.

ExxonMobil Aviation International Ltd. . ExxonMobil Aviation: World Jet Fuel Specifications with Avgas Supplement 2005 Edition. Leatherhead, UK: ExxonMobil Aviation International Ltd; 2005.

Giannetto G, Monque R, Galiasso R. Transformation of LPG into aromatic hydrocarbons and hydrogen over zeolite catalysts. Catal Rev Sci Eng 1994;36(2):271–304.

Grossmann IE, Westerberg AW. Research challenges in process systems engineering. AIChE J 2000;46(9):1700–3.

Hui X, Kumar K, Sung CJ, Edwards T, Gardner D. Experimental studies on the combustion characteristics of alternative jet fuels. Fuel 2012;98:176–82.

Kazansky VB, Frash MV, Van Santen RA. A quantum-chemical study of hydride transfer in catalytic transformations of paraffins on zeolites. Pathways through adsorbed nonclassical carbonium ions. Catal Lett 1997;48(1–2):61–7.

Knothe G. Biodiesel and renewable diesel: a comparison. Prog Energy Combust Sci 2010;36(3):364–73.

Lam HL, Klemeš JJ, Kravanja Z, Varbanov PS. Software tools overview: process integration, modelling and optimisation for energy saving and pollution reduction. Asia Pac J Chem Eng 2011;6(5):696–712.

Li J, Ge W, Zhang J, Kwauk M. Multiscale compromise and multi-level correlation in complex systems. Chem Eng Res Des 2005;83(6):574–82.

Lukyanov DB, Gnep NS, Guisnet MR. Kinetic modeling of ethene and propene aromatization over HZSM-5 and GaHZSM-5. Ind Eng Chem Res 1994;33(2):223–34.

Lukyanov DB, Gnep NS, Guisnet MR. Kinetic modeling of propane aromatization reaction over HZSM-5 and GaHZSM-5. Ind Eng Chem Res 1995;34(2):516–23.

Morales-Rodríguez R, Gani R, Déchelotte S, Vacher A, Baudouin O. Use of CAPE-OPEN standards in the interoperability between modelling tools (MoT) and process simulators (Simulis® Thermodynamics and ProSimPlus). Chem Eng Res Des 2008;86(7):823–33.

Morales-Rodríguez R, Gani R. Computer-aided multiscale modelling for chemical process engineering. Comput Aided Chem Eng 2007;24:207–12.

Nguyen LH, Vazhnova T, Kolaczkowski ST, Lukyanov DB. Combined experimental and kinetic modelling studies of the pathways of propane and n-butane aromatization over H-ZSM-5 catalyst. Chem Eng Sci 2006;61(17):5881–94.

Pirola C, Manenti F, Galli F, Bianchi CL, Boffito DC, Corbetta M. Heterogeneously catalyzed free fatty acids esterification in (monophasic liquid)/solid Packed Bed Reactors (PBR). Chem Eng Trans 2014;37:553–8.

Platts. McGraw Hill Financial; 2014 http://www.platts.com/

Shu J, Adnot A, Grandjean BP. Bifunctional behavior of Mo/HZSM-5 catalysts in methane aromatization. Ind Eng Chem Res 1999;38(10):3860–7.

Visconti C, Lietti L, Manenti F, Daturi M, Corbetta M, Pierucci S, et al. Spectrokinetic analysis of the NOx storage over a Pt–Ba/Al2O3 lean NOx trap catalyst. Top Catal 2013;56:311–6.

Wang J, Kang M, Zhang Z, Wang X. Propane aromatization over Mo/HZSM-5 catalysts. J Nat Gas Chem 2002;11(1):43–50.